International Journal of Automotive Technology, Vol. 21, No. 1, pp. 181−188 (2020)
DOI 10.1007/s12239−020−0018−7

pISSN 1229−9138/ eISSN 1976−3832

INTERNAL CAVITATING FLOW AND EXTERNAL SPRAY BEHAVIOR CHARACTERISTICS ACCORDING TO LENGTH-TO-WIDTH RATIO OF TRANSPARENT NOZZLE ORIFICE

Seungcheon Ro[1)], Byunggyun Kim[2)], Suhan Park[3)*], Young-Bae Kim[3)], Byungchul Choi[3)], Seunghun Jung[3)] and Dong-Weon Lee[3)]

[1)]Transportation Pollution Research Center, National Institute of Environmental Research, 42 Hwangyeong-ro, Seo-gu, Incheon 22689, Korea
[2)]Department of Mechanical Engineering, Graduate School of Chonnam National University, Gwangju 61186, Korea
[3)]School of Mechanical Engineering, Chonnam National University, Gwangju 61186, Korea

(Received 4 October 2018; Revised 14 December 2018; Accepted 18 June 2019)

ABSTRACT−The purpose of this study is to investigate effects of length-to-width (L/W) ratio on cavitation flow inside a transparent acrylic nozzle orifice, and its effects on spray angle. Three visualization nozzles with different geometries (L/W = 2.0, 2.67, and 4.0) are used, and the working fluid is water. In order to visualize the development process of cavitation, the injection pressure of the working fluid is changed, and a high-speed camera is used with a metal-halide lamp. From experiments and analysis, some important facts are determined. As the injection pressure increases, the cavitation length and thickness increase linearly until the hydraulic flip occurs. Although the cavitation width varies according to the orifice width, the maximum cavitation thickness relative to the orifice width is almost constant at approximately 25 % ~ 30 %. When the nozzle shape ratio increases, the discharge coefficient tends to increase because of the decrease in friction area. When entering the hydraulic flip region, the discharge coefficient decreases due to the reduction of the exit section area. The spray angle is affected by the cavitation number, cavitation length, cavitation thickness, and Reynolds number. The higher the injection pressure, the higher the turbulence intensity, and the greater the instability of the fluid flow.

KEY WORDS : Length-to-width ratio, Cavitation, Hydraulic flip, Spray angle, Discharge coefficient, Cavitation number

NOMENCLATURE

CN : cavitation number
L/W : length-to-width
P : pressure
Re : reynolds number

SUBSCRIPT

inj : injection

1. INTRODUCTION

The formation process and uniformity of the air-fuel mixture supplied in a combustion chamber greatly affects its combustion performance and emissions characteristics. Hence, in order to form a uniform mixture, various attempts, such as reducing nozzle hole size, and increasing injection pressure, have been performed. Pang *et al*. (2017) reported that large nozzle hole size, such as 100 μm, 180 μm, and 363 μm, increase the amount of fuel injected, creating a rich equivalence ratio level and, finally, adversely affecting spray flame retardation due to the deterioration of uniformity of the mixture. Su *et al*. (1995) reported that the Sauter mean diameter (SMD) of a sharp-edged nozzle is larger than that of a rounded-edged nozzle, and the higher injection pressure induced a small SMD in the study on the atomization characteristics according to the shape of the nozzle inlet and injection pressure. Meanwhile, as the injection pressure increases, the fluid flow instability inside the injector nozzle is increased. When the fluid passes through a narrow-sectional orifice under the high injection pressure condition, a vena contracta is formed that fails to flow along the corner shape of the nozzle orifice inlet and causes the cross-section area of flow to narrow. As the fluid passes through the area of the vena contracta of the narrow flow path, the dynamic pressure increases, and the static pressure decreases. If the static pressure is lower than the vapor pressure of the fluid, bubbles in the fluid occur, which is called cavitation. Depending on the pressure conditions, cavitating flow, which is a two-phase flow in which bubbles grow and liquid- and gas-phases coexist, grows along the wall, and sometimes up to the nozzle outlet. Bubbles grow and

**Corresponding author*: e-mail: suhanpark@jnu.ac.kr

explode as the pressure changes in the orifice, and shock energy released outside when bubbles explode is known to promote liquid atomization (Mauger *et al*., 2012; Prabhakar *et al*., 2013; Wang *et al*., 2015). As the injection pressure becomes high, the generation and development of cavitation flow is inevitable.

Various studies have been actively conducted, including studies on the generation and development of cavitation flow, and its effect on spray and atomization characteristics. Sou *et al*. (2007) studied cavitation characteristics using a two-dimensional acrylic nozzle and divided the results into four areas, such as no cavitation / developing cavitation, super cavitation and hydraulic flip, according to the characteristics of the cavitation flow. In addition, Sou *et al*. (2008a) reported that the formation of a ligament, which is an intermediate stage of fluid breakup, is affected by the collapse of the cavitation cloud on the nozzle wall from a cylindrical nozzle. They also conducted a cavitation bubble visualization study using an X-ray light source (Sou *et al*., 2015), and found that the cavitation bubble does not maintain a spherical shape, depending on the nozzle size and the structure of the flow detachment. He and Ruiz (1995) measured the speed of cavitating flow and non-cavitating flow inside a two-dimensional nozzle using laser Doppler velocimetry (LDV). The results showed that the average flow rate and turbulence were high for cavitation flow. Chaves and Schuhbauer (2006) produced two asymmetrically sized acrylic nozzles of the same size and an actual diesel injector with valve covering orifice (VCO) type nozzles and compared them to axial ball injectors. They revealed that the asymmetry of the nozzle hole is closely related to the generation of vortexes and cavitation. Mitroglou *et al*. (2011) revealed that the structure of string cavitation is related to injection instability. Pratama and Sou (2013) analyzed the occurrence timing of string cavitation in accordance with the injector needle position. They reported that the lower the needle position in a cylindrical nozzle, the greater the injection angle, and the greater the string cavitation. As shown in the results of the preceding studies, the cavitation is mainly affected by the nozzle shape (geometry), length-to-diameter (L/D) ratio, inlet angle of the nozzle orifice, and the Reynolds number (Sou *et al*., 2008b), as well as the nozzle orifice inlet roundness, the behavior of injector needle, the surface roughness inside nozzle orifice, and fuel properties.

The purpose of this study is to find out how the geometric shape of the nozzle affects the generation of the cavitation and the effect of the cavitation on the fluid injection. Most cavitation experiments based on L/W conditions are carried out by changing the nozzle length conditions. However, in this study, the length of the nozzle orifice is fixed, and the width is changed in order to change the nozzle shape ratio (length-to-width (L/W) ratio). Because the diameter of the injector nozzle gradually become small in order to improve atomization, the nozzle width was changed in this experiment. In addition, the effect of cavitation on spray behavior and spray angle was investigated by simultaneously visualizing the inside and outside of the nozzle.

2. EXPERIMENTAL APPARATUS SET-UP AND PROCEDURE

Figure 1 (a) shows a schematic diagram of the experimental devices for visualizing the internal- and the external-flow of a transparent acrylic nozzle. The water was used as the working fluid, and it was supplied by adjusting to 0.1 bar using inverter pumps, as shown in Figure 1 (b). The flow rate of the working fluid was measured in real time by installing an instantaneous flow meter (DY-L15, Flstronic) between the pump and the acrylic nozzle. The fluid passing through the acrylic nozzles was stored in reservoir tank A and moved to reservoir tank B for supplying the working fluid through an underwater pump for the circulation system. An ultra-high speed camera (FASTCAM Mini AX100, Photron, Tokyo, JP) was installed on the front of the acrylic nozzle, and a 250W metal-halide lamp (MID-25FC, Kyowa Co. Ltd, Osaka, JP) and filter paper were installed on the back in order to visualize the internal and external flow using the shadow graph visualization technique. Table 1 shows the experimental conditions and properties of the water.

Figure 2 shows a design sketch of the acrylic (PMMA) nozzle used in the experiment and the actual acrylic nozzle

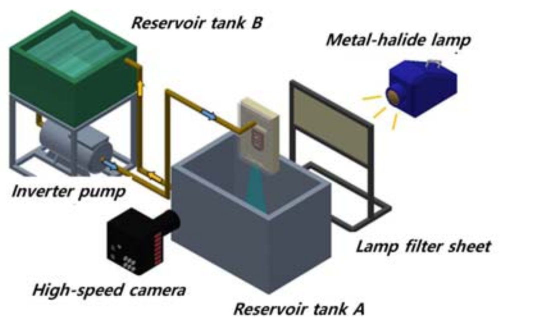

(a) Schematic diagram of experimental apparatus for visualization of internal- and external-flow characteristics

(b) Pump for supplying water and reservoir

Figure 1. Schematic diagram of experimental apparatus and picture for pump and reservoir.

Table 1. Experimental conditions and Properties of working fluid.

Length-to-width (L/W) ratio		4.0 (L = 8, W = 2) 2.67 (L = 8, W = 3) 2.0 (L = 8, W = 4)
Injection pressure (bar)		1.0 ~ 3.0 (step 0.1)
Ambient pressure (bar)		1
Working fluid	Fluid	Tap water
	Density	998 kg/m^3
	Kinematic viscosity @20 ℃	1.0038 m^2/s

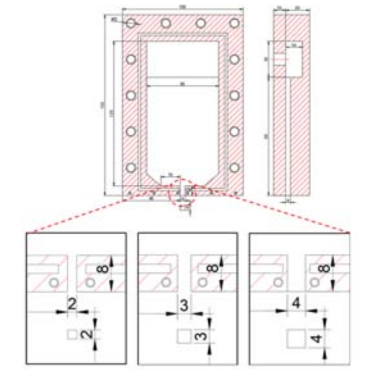

(a) Design sketch of test nozzle with size

(b) Picture of three test nozzles

Figure 2. Design sketch and pictures of three test nozzles.

photograph. Three test nozzles having nozzle shape (L/W) ratios of 4.0, 2.67, and 2.0 were manufactured by holding the hole length at 8 mm and changing the width to 2 mm ~ 4 mm. The criteria of term of "nozzle shape (L/W) ratios" is as follows. Firstly, we used the average value of the commercial GDI injector L/D. Secondly, to confirm the change in the cavitating flow according to the L/W change by varying the nozzle thickness by 1 mm while holding the nozzle length as a fixed variable in L/W. Thirdly, due to limitations in manufacturing technology, the minimum value of W change was 1 mm. The thickness of the nozzle was minimized as much as possible to observe the internal

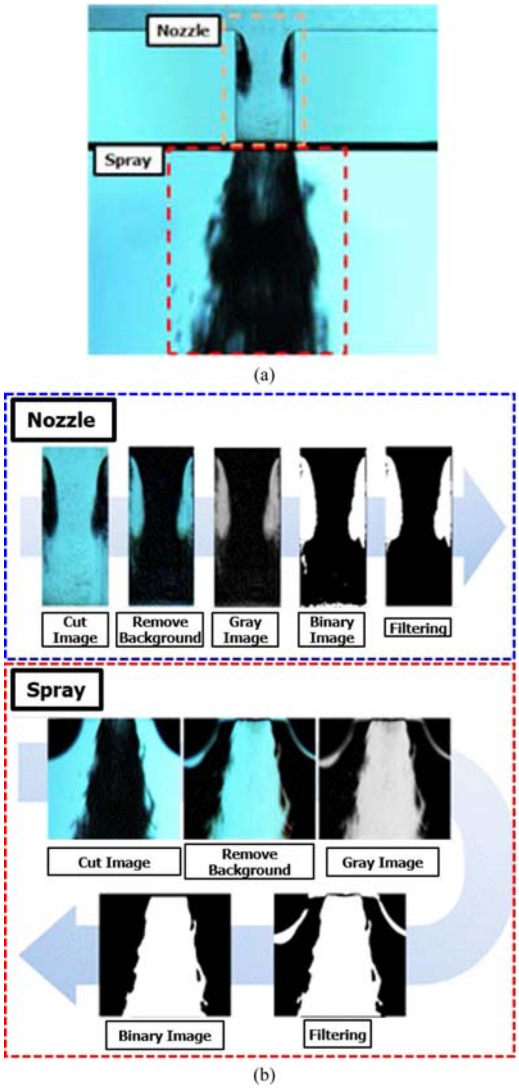

Figure 3. Sample image (a) and flow chart of image processing (b).

flow as well as, the generation and development of cavitation. In addition, to simulate the maximum open injector needle, a needle was installed 30 mm away from the acrylic nozzle hole, and fluid was supplied symmetrically from the left and right sides.

Figure 3 shows the image post-processing process of acquired cavitation flow and spray images. Figure 3 (a) is an image showing the inside and outside of the nozzle taken by the shadow technique, and Figure 3 (b) shows the sequence diagram showing the post-processing of the image for analyzing cavitation flow inside the nozzle and external spray. The images taken with the internal cavitation and development phenomenon of the nozzle and external flow were quantified using image processing, such as removing the background and converting to black-and-white images through binarization.

Figure 4 describes the definition of the spray angle of the

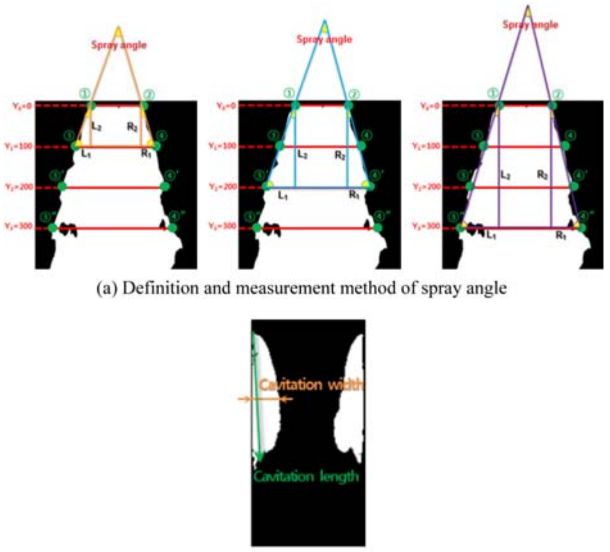

(a) Definition and measurement method of spray angle

(b) Definition of cavitation width and length

Figure 4. Definition of spray angle, cavitation width, and cavitation length.

external spray and the cavitation thickness. Figure 4 (a) represents the method of measuring the spray angle from the binarized image, and Figure 4 (b) is intended to describe the definition of the cavitation length and thickness. The spray angle of fluid injected from the nozzle can be obtained from the calculation of angles ∠③ (③′, ③″) and ∠④ (④′, ④″) through the equation of the triangle function at the end of the nozzle exit (Y0) and at 100 mm (Y_1), 200 mm (Y_2), and 300 mm (Y_3). The remaining angle of the triangle formed by ∠③ and ∠④ are defined by the spray angle. The mean value of the three spray angles, calculated at points 100 mm, 200 mm, and 300 mm, was used. The cavitation length was defined as the distance from the beginning of the cavitation and the thickness of the cavitation was defined as the equidistant measurement point within the nozzle.

This study also used two dimensionless numbers the cavitation number (CN) and the Reynolds number (Re) which are defined as follows:

$$CN = \frac{P_{inj} - P_{amb}}{P_{amb} - P_{vapor}} \quad (1)$$

$$Re = \frac{\rho VD}{\mu} = \frac{VD}{\nu} \quad (2)$$

where P_{inj}, P_{amb}, and P_{vapor} are the injection pressure, the ambient pressure, and the vapor pressure of the working fluid (water), respectively; and ρ, V, D, and ν are the fluid density, the fluid velocity, the width of nozzle orifice, and the kinematic viscosity, respectively. In general, the vapor pressure can be ignored because it is very small compared to the injection pressure and the atmospheric pressure. The cavitation number (CN) is representative of the strength of the cavitation (Lindström, 2009).

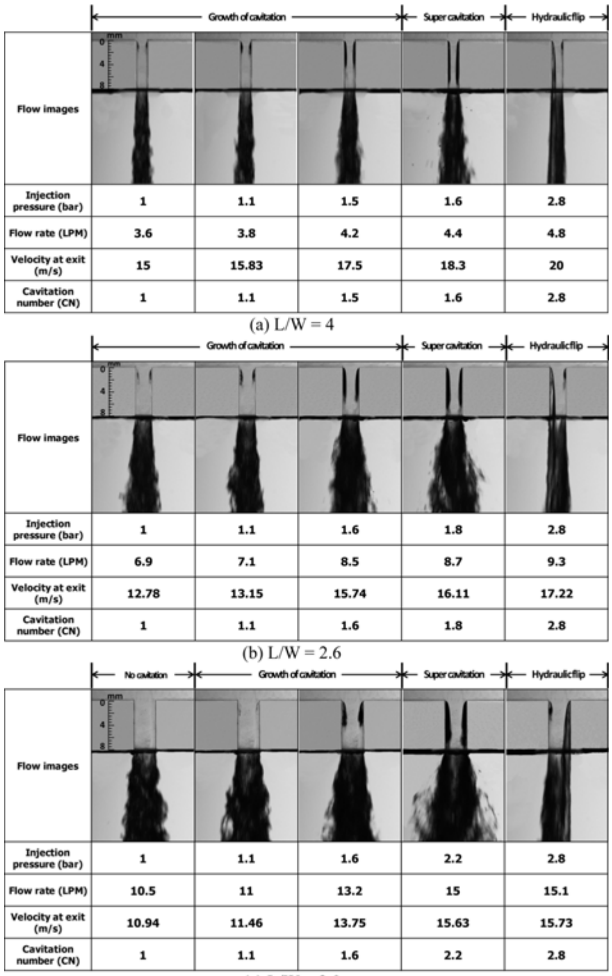

Figure 5. Cavitation development process according to injection pressure and L/W (length-to-width) ratio.

3. RESULTS AND DISCUSSION

3.1. Effect of Injection Pressure on Cavitation Growth

Figure 5 shows the generation and growth process of the cavitation according to the injection pressure in three acrylic nozzles with different nozzle shape ratios. Depending on the generation and growth of the cavitation, it can be divided into areas of "No cavitation", "Growth of cavitation (including generation)", "Super cavitation", and "Hydraulic flip". Generally, when defining the cavitating flow, the "No cavitation", and "hydraulic flip" are clearly distinguished. However, the "Growth of cavitation" and "super cavitation" differ according to the authors' standards. We defined the "Growth of cavitation" up to before the "super cavitation" region. Here, the "super cavitation" is defined as a case where the cavitation has grown by 70 to 80 %. As shown in Figure 5, under the 1 bar injection pressure condition, there is no cavitation in

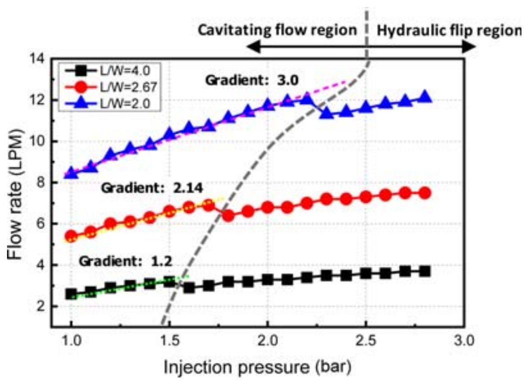

Figure 6. Flow rate characteristics for L/W ratio and injection pressure.

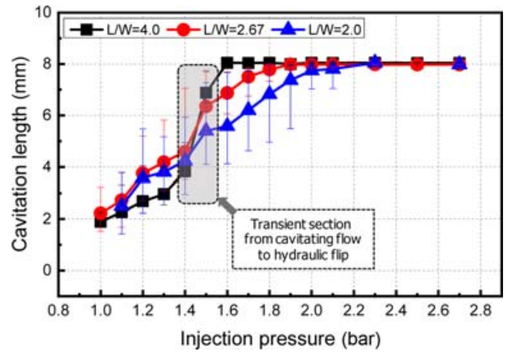

Figure 7. Cavitation length for the L/W ratio and injection pressures.

the L/W = 2 nozzle (Figure 5 (c)), but it was observed that the cavitation was formed in the L/W = 2.67 and 4.0 nozzles (Figures 5 (a) and (b)). A large nozzle shape ratio in this study means that the nozzle width (W) is small. Therefore, even under the same injection pressure conditions, the fluid will pass through a narrower flow path, the flow rate will be reduced, and the static pressure will be reduced faster, resulting in an early formation of cavitation. In addition, as the injection pressure increases, the cavitation area within the orifice becomes larger and continues to grow until both cavitation length and thickness reach the nozzle exit. When the cavitation reaches the nozzle exit, it enters the hydraulic flip, reducing the atomization characteristics of the cavitation flow (Park *et al*., 2008), and dramatically reduces the injection angle. As the cavitation occurs first at nozzles with large nozzle shape ratios, the growth rate of the cavitation and the timing of entry into the hydraulic flip area are also rapidly shown. As the injection pressure increases, the flow rate and the CN increases, and the cavitation flow become active by the increase of cavitation length in the nozzle. When the cavitation flow becomes active, the growth of the air bubbles and their explosion will have a greater effect on liquid atomization, which will result in a greater injection angle of fluid injected from the nozzle exit. Therefore, the spray angle of fluid injected during the super cavitation phase is greatest.

Figure 6 shows the flow rate characteristics according to nozzle shape ratio and injection pressure. While the flow rate increases linearly as the injection pressure increases in the areas of cavitation generation and growth (cavitating flow region), the flow rate decreases slightly in the hydraulic flip phases because the working fluid (water) in not reattached to the orifice wall but is injected through the reduced exit area. When comparing the increasing rate of flow rate, it was found that the smaller the nozzle shape ratio, the higher the increasing rate of flow rate. Because this indicates that the width of the nozzle is larger, the increase of the flow rate for a nozzle that has a larger cross-sectional area that passes through the fluid is high.

Figure 7 shows a graph comparing the cavitation length with the injection pressure. As shown in the figure, the cavitation length gradually increases as the injection pressure increases, and as it grows to the end of the nozzle, it enters the hydraulic flip area and maintains a constant cavitation length. Specifically, when the injection pressure was increased from 1.4 bar to 1.5 bar, it was found that the cavitation length increased rapidly in all three nozzles. In addition, the larger the nozzle shape ratio, the faster the cavitation length is growing, with the first growth to the end of the nozzle, and the result was that it entered the hydraulic flip phase. As described earlier, because acrylic nozzles used in this experiment have a fixed orifice length and change in width to yield various nozzle shape ratios, a larger nozzle shape ratio means a smaller nozzle width. The larger the nozzle shape, the larger the pressure drop to lower pressure than the saturated vapor pressure, and the greater the cavitation will occur first. In other word, the larger the nozzle shape ratio, the faster the cavitation occurs, and the faster it grows to the end of the nozzle orifice.

Figure 8 shows a graph comparing the cavitation width, cavitation width ratio, and length for the condition where the cavitation has grown to the maximum inside the three

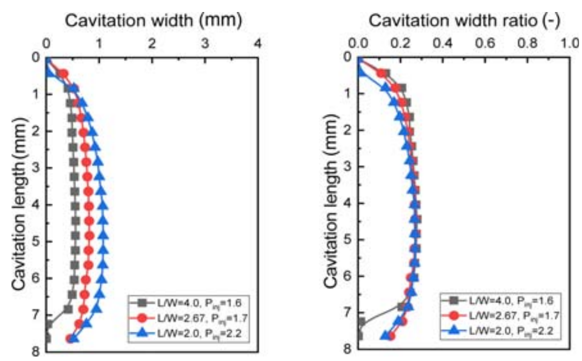

Figure 8. Cavitation length, cavitation width ratio, and coefficient of contraction (C_c) according to L/W ratio at super cavitation condition.

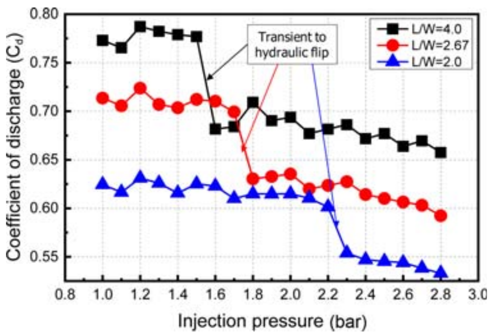

Figure 9. Discharge coefficient (C_d) characteristics for L/W ratio and injection pressure.

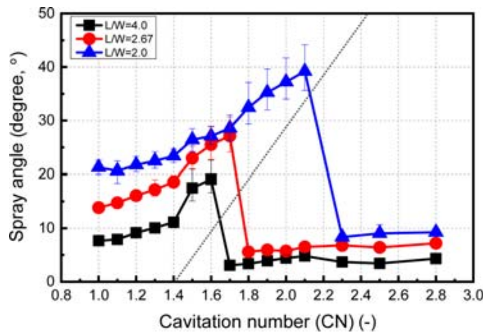

Figure 10. Spray angle characteristics for cavitation number at different L/W ratio nozzles.

acrylic nozzles. Cavitation width data was acquired with average value of the acquired 100 images values was used. Figure 8 (a) is the actual measurement value of cavitation width and length. The cavitation ratio in Figure 8 (b) means the relative value of cavitation width for the orifice width. When comparing the cavitation width, such as in Figure 8 (a), the larger the nozzle width (smaller the nozzle shape ratio), the greater the cavitation width. However, compared with the cavitation width ratio relative to the orifice width of nozzle, the result commonly account for approximately 25 % ~ 30 % of the orifice width. Under high injection pressure, when the fast fluid enters a rapidly narrowing flow path, it fails to follow the shape of the corner of the orifice and forms a vena contracta that narrows the flow path. The rate at which the orifice width is contracted to the width of the vena contracta is referred to as the coefficient of contraction (C_c). In general, C_c is set at 0.61 ~ 0.64 depending on the orifice entrance slope angle. Therefore, the width of the vena contracta relative to the orifice width is generally constant; hence, the ratio of cavitation width is considered constant regardless of the orifice width. The maximum cavitation width ratio was found to be greatest at 4 ~ 5 mm (around the center point of the nozzle orifice) in three test nozzles.

Figure 9 shows the coefficient of discharge (C_d) with the injection pressure. The C_d represents the ratio of the actual flow rate to the calculated flow rate as follows.

$$C_d = \frac{\dot{m}}{A\sqrt{2\Delta P/\rho}} \tag{3}$$

where A is the cross-section area of the nozzle exit, ΔP is the pressure difference, ρ is the density of working fluid, and $\dot{m}$ is the actual flow rate. In Figure 9, all three nozzles show a sharp decrease in flow rate due to the narrowing of the exit cross section when entering the hydraulic flip area from the cavitation area. In addition, the higher the nozzle shape ratio, the higher is C_d. Due to the nozzle characteristics used in the experiment, the section area of the exit is narrow because the width of the orifice is smaller. Because the friction area that affects flow is smaller when the exit area is reduced, it is believed that the flow coefficient is high. It can be seen that the flow rate decreases gradually when the injection pressure has increased after the onset of hydraulic flip. In the hydraulic flip region, the external air entered the empty space between the orifice wall and the fluid inside the nozzle. When the injection pressure increases, the relative velocity of injection spray for the ambient air also increases. Then, the air entrainment into the orifice improves, and the effective exit cross area is decreased. Consequently, the discharge coefficient will decrease.

3.2. Injection Angle Characteristics according to the Growth of Cavitation

The cavitation formed and grown inside the nozzle orifice also has a significant effect on the spray behavior and atomization. In this section, we analyze how the cavitation flow characteristics that occur inside the nozzle affect the spray angle characteristics outside the nozzle.

Figure 10 shows a graph comparing the spray angle with the variation of the cavitation number in the three test nozzles. As expressed in Equation (1), the injection pressure and ambient pressure are important factors in CN; the increase of injection pressure causes the linear increase of CN. Comparing the spray angle according to the CN, as in Figure 10, the spray angle in the region of cavitation formation increases linearly with the CN, however, when the phenomenon of cavitation enters the hydraulic flip region, the spray angle decreases rapidly compared to the maximum injection angle. After that, it can be observed that the spray angle does not change significantly, even if CN increase. In the cavitation region, an increase of the spray angle resulting from an increase in the velocity of working fluid (i.e., an increase in the CN) can be explained as follows. First, the fluid breakup is actively carried out as the relative velocity between the injected fluid and ambient air increases with the increase of fluid velocity (Hiroyasu, 2000). Second, during the cavitating bubble explosion inside the flow, the energy released outward influences the atomization of the fluid, which results in a larger spray angle (Magnotti *et al*., 2018). As the cavitation develops to the end of the orifice, it enters the hydraulic flip region

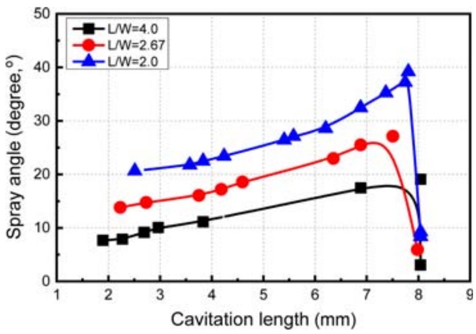

Figure 11. Spray angle characteristics for cavitation length at different L/W ratio nozzles.

where the outer gas fills the area occupied by the cavitation, disintegrating and leaving only the cavitation on one-side wall. This reduces the effect of cavitation on atomization, resulting in longer breakup lengths and reduced spray angle. As shown in Figure 8, although the cavitation width is constant against the nozzle width, the lower the nozzle shape ratio, the thicker the cavitation width becomes and the larger the area the cavitation takes. Therefore, the lower the nozzle shape ratio, the higher the instability of the shrinking area and fluid flow caused by the cavitation, and the greater the spray angle and the greater the refinement. Meanwhile, the spray angles were found to decrease as the nozzle shape ratio increased under the same CN.

Figure 11 shows the variation in the spray angle along the cavitation length. The longer the cavitation length, the greater the degree of atomization caused by the cavitation phenomenon, indicating a greater injection angle. When the cavitation is 8 mm long and reaches the end of nozzle orifice, the fluid enters the hydraulic flip region, and the injection angle decreases rapidly. The longer the cavitation length, the longer the fluid passing through the nozzle is expected to be affected by the cavitation for a significant time, and the greater the injection angle. In addition, as the cavitation is extended near the nozzle exit, the area of the vena contracta is also extended, extending the distance through the constricted passage and increasing the speed. It is believed that rapid discharge of fluid from the outside resulted in increased friction with the surrounding atmosphere, resulting in improved atomization.

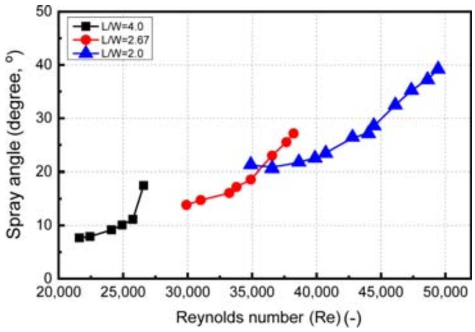

Figure 12. Relationship between spray angle and Reynolds number for three different test nozzles.

Figure 12 shows a graph that analyzes the spray angle according to Re at each nozzle. Comparing the spray angle according to Re, it was found that the spray angle increased as Re increased, regardless of the nozzle shape ratio. Even under the same injection pressure conditions, the distribution range of Re for each nozzle is clearly distinct because the orifice width and the injection velocity are different. The smaller the nozzle shape ratio, the greater the distribution range of Re for the formation and growth of cavitation. It is well known that the turbulence intensity is to be stronger and fluid flow unstable as Re increases. Therefore, it is considered that the increase in Re shortened the breakup length and increased the spray angle.

4. CONCLUSION

In this paper, the characteristics of cavitation flow (generation and growth) and their effect on spray angle were investigated under various injection pressure conditions by using transparent rectangular acrylic nozzles with different nozzle shape ratios (L/W ratio). From the experimental results and discussion, we derived the following conclusions.

(1) In the cavitation flow region, the flow rate increases linearly with an increase in the injection pressure. When the flow enters the hydraulic flip region, the flow rate decreases due to the reduction of the exit cross section. Next, the flow rate increases along with the injection pressure.
(2) The larger the nozzle shape ratio, the larger the pressure drop due to a change in the section area. This results in lower pressures for the generation of cavitation and entry into the hydraulic flip region.
(3) As the injection pressure increases, the cavitation length and width increase linearly until the hydraulic flip occurs. Although the cavitation width varies according to the orifice width, the maximum cavitation width relative to the orifice width is almost constant at approximately 25 % ~ 30 %.
(4) When the nozzle shape ratio increases, the discharge coefficient tends to increase because of the decrease in friction area. When entering the hydraulic flip region, the discharge coefficient decreases due to the reduction in the exit section area.
(5) The spray angle is affected by the cavitation number, cavitation length, cavitation width, and Reynolds number. The higher the injection pressure, the higher the turbulence intensity, and the greater the instability of the fluid flow. In addition, the greater the length and width of cavitation, the larger the area of the fluid exposed to the cavitation bubble explosion, and the better the atomization by the cavitation.

ACKNOWLEDGEMENT–This study was financially supported by the Basic Science Research Program (2016R1D1A3B03935537) and Basic Research Laboratory Program (2015R1A4A1041746) through the National Research Foundation of Korea (NRF) funded by the Ministry of Education of Korea.

REFERENCES

Chaves, H. and Schuhbauer, I. (2006). Cavitation in an asymmetric transparent real-size VCO nozzle. *Spray'06, Workshop uber Sprays, Erfassung von Spruhvorgangen und Techniken der Fluidzerstaubung.*

He, L. and Ruiz, F. (1995). Effect of cavitation on flow and turbulence in plain orifices for high-speed atomization. *Atomization Sprays* **5**, **6**, 569–584.

Lindström, M. (2009). *Injector Nozzle Hole Parameters and Their Influence on Real DI Diesel Performance*. Ph. D. Dissertation. KTH. Stockholm, Sweden.

Mauger, C., Méès, L., Michard, M., Azouzi, A. and Valette, S. (2012). Shadowgraph, Schlieren and interferometry in a 2D cavitating channel flow. *Experiments in Fluids* **53**, **6**, 1895–1913.

Mitroglou, N., Gavaises, M. and Arcoumanis, C. (2011). Cavitation inside enlarged and real-size fully transparent injector nozzles and its effect on near nozzle spray formation. *Proc. DIPSI Workshop*, Bergamo, Italy.

Pang, K. M., Jangi, M., Bai, X.-S., Schramm, J. and Walther, J. H. (2017). Effects of nozzle diameter on diesel spray flames: A numerical study using an eulerian stochastic field method. *Proc. 9th Int. Conf. Applied Energy*, Cardiff, UK.

Park, S. H., Suh, H. K. and Lee, C. S. (2008). Effect of cavitating flow on the flow and fuel atomization characteristics of biodiesel and diesel fuels. *Energy Fuels* **22**, **1**, 605–613.

Prabhakar, B. S., Laxmanrao, S. P. and Salim, K. J. A. M. (2013). Investigation of atomization and cavitation characteristics in nozzle. *Int. J. Innovative Research in Science, Engineering and Technology* **2**, **11**, 6200–6206.

Pratama, R. H. and Sou, A. (2013). String cavitation in a fuel injector. *Proc. 16th Annual Conf. Institute for Liquid Atomization and Spray Systems-Asia*, Nagasaki, Japan.

Sou, A., Hosokawa, S. and Tomiyama, A. (2007). Effects of cavitation in a nozzle on liquid jet atomization. *Int. J. Heat and Mass Transfer* **50**, **17-18**, 3575–3582.

Sou, A., Maulana, M. I., Hosokawa, S. and Tomiyama, A. (2008a). Ligament formation induced by cavitation in a cylindrical nozzle. *J. Fluid Science and Technology* **3**, **5**, 633–644.

Sou, A., Maulana, M. I., Isozaki, K., Hosokawa, S. and Tomiyama, A. (2008b). Effects of nozzle geometry on cavitation in nozzles of pressure atomizers. *J. Fluid Science and Technology* **3**, **5**, 622–632.

Sou, A., Minami, S., Prasetya, R., Pratama, R. H., Moon, S., Wada, Y. and Yokohata, H. (2015). X-ray visualization of cavitation in nozzles with various sizes. *Proc. 13th Triennial Int. Conf. Liquid Atomization and Spray Systems*, Tainan, Taiwan.

Hiroyasu, H. (2000). Spray breakup mechanism from the hole- type nozzle and its applications. *Atomization and Sprays* **10**, **3**, 511–527.

Magnotti, G. M., Battistoni, M., Saha, K. and Som, S. (2018). Evaluation of a new cavitation erosion metric based on fluid-solid energy transfer in channel flow simulations. *Proc. 14th Triennial Int. Conf. Liquid Atomization and Spray Systems*, Chicago, Illinois, USA.

Su, T. F., Chang, C. T., Reitz, R. D., Farrell, P. V., Pierpont, A. D. and Tow, T. C. (1995). Effects of injection pressure and nozzle geometry on spray SMD and DI emissions. *SAE Paper No*. 952360.

Wang, F., He, Z., Liu, J. and Wang, Q. (2015). Diesel nozzle geometries on spray characteristics with a spray model coupled with nozzle cavitating flow. *Int. J. Automotive Technology* **16**, **4**, 539–549.